Acta Pharmaceutica Sinica B 2022;12(2):665−677

Chinese Pharmaceutical Association
Institute of Materia Medica, Chinese Academy of Medical Sciences

Acta Pharmaceutica Sinica B

www.elsevier.com/locate/apsb
www.sciencedirect.com

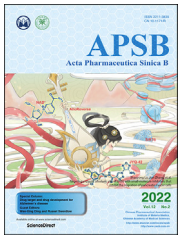

ORIGINAL ARTICLE

Anti-aging effects of chlorpropamide depend on mitochondrial complex-II and the production of mitochondrial reactive oxygen species

Zhifan Mao[a,†], Wenwen Liu[a,†], Yunyuan Huang[a], Tianyue Sun[a], Keting Bao[a], Jiali Feng[a], Alexey Moskalev[b], Zelan Hu[a,*], Jian Li[a,c,d,*]

[a]*State Key Laboratory of Bioreactor Engineering, Frontiers Science Center for Materiobiology and Dynamic Chemistry, Shanghai Key Laboratory of New Drug Design, East China University of Science and Technology, Shanghai 200237, China*
[b]*Laboratory of Geroprotective and Radioprotective Technologies, Institute of Biology, Komi Science Centre, Ural Branch, Russian Academy of Sciences, Syktyvkar 167982, Russia*
[c]*Yunnan Key Laboratory of Screening and Research on Anti-pathogenic Plant Resources from West Yunnan, College of Pharmacy, Dali University, Dali 671000, China*
[d]*Clinical Medicine Scientific and Technical Innovation Center, Shanghai Tenth People's Hospital, Tongji University School of Medicine, Shanghai 200092, China*

Received 23 May 2021; received in revised form 22 July 2021; accepted 30 July 2021

KEY WORDS

Sulfonylureas;
Chlorpropamide;
Anti-aging;
Mitochondrial complex II;
Mitochondrial reactive oxygen species;
ATP sensitive potassium channels;
Senescence;
Succinate dehydrogenase

Abstract Sulfonylureas are widely used oral anti-diabetic drugs. However, its long-term usage effects on patients' lifespan remain controversial, with no reports of influence on animal longevity. Hence, the anti-aging effects of chlorpropamide along with glimepiride, glibenclamide, and tolbutamide were studied with special emphasis on the interaction of chlorpropamide with mitochondrial ATP-sensitive K^+ (mitoK-ATP) channels and mitochondrial complex II. Chlorpropamide delayed aging in *Caenorhabditis elegans*, human lung fibroblast MRC-5 cells and reduced doxorubicin-induced senescence in both MRC-5 cells and mice. In addition, the mitochondrial membrane potential and ATP levels were significantly increased in chlorpropamide-treated worms, which is consistent with the function of its reported targets, mitoK-ATP channels. Increased levels of mitochondrial reactive oxygen species (mtROS) were observed in chlorpropamide-treated worms. Moreover, the lifespan extension by chlorpropamide required complex II and increased mtROS levels, indicating that chlorpropamide acts on complex II directly or

*Corresponding authors.
E-mail addresses: jianli@ecust.edu.cn (Jian Li), huzelan@ecust.edu.cn (Zelan Hu).
†These authors made equal contributions to this work.
Peer review under responsibility of Institute of Materia Medica, Chinese Academy of Medical Sciences and Chinese Pharmaceutical Association.

https://doi.org/10.1016/j.apsb.2021.08.007

indirectly *via* mitoK-ATP to increase the production of mtROS as a pro-longevity signal. This study provides mechanistic insight into the anti-aging effects of sulfonylureas in *C. elegans*.

1. Introduction

Sulfonylureas were the first oral hypoglycemic drugs used clinically for the treatment of type 2 diabetes mellitus and have still been widely used due to their efficacy and affordability[1]. Although the meta-analyses of different clinical data reveal the effects of prolonged use of sulfonylureas on the patient's lifespan are controversial, no studies have described the effect of sulfonylureas on animal longevity[2]. In our screening of anti-aging drug candidates using *Caenorhabditis elegans* as an animal model for the evaluation of lifespan extension, some sulfonylureas including chlorpropamide, glimepiride, glibenclamide, and tolbutamide were found to extend the lifespan of *C. elegans*. This aroused our interest in studying how sulfonylureas affect the aging process.

Sulfonylureas exert their anti-diabetic effects by inhibiting ATP-sensitive K^+ (K-ATP) channels in the plasma membrane of islet β-cells[3,4]. In 1991, K-ATP channels have also been reported to be located in the inner membrane of mitochondria[5]. But, the existence of mitochondrial K-ATP (mitoK-ATP) channels was a matter of debate, until the protein complex of mitoK-ATP channel was identified recently[6]. MitoK-ATP channel, which is composed of a channel-forming subunit (MITOK) and a regulatory subunit that carries the ATP-binding domain (MITOSUR), has similar properties of those K-ATP channels on plasma. It can be inactivated by ATP and glibenclamide[7], and activated by diazoxide[8]. In mitochondria, mitoK-ATP channel work with other electrophoretic K^+ pores and K^+/H^+ exchange transporters to maintain potassium homeostasis[9]. This balance help maintain proper mitochondrial volume and protonmotive force (Supporting Information Fig. S1). MitoK-ATP channel is also reported to be activated when mitochondrial metabolism is inhibited[10] and its activation is thought to mediate preconditioning protection effect[11], indicating its role in stress resistance.

Mitochondrial complex II, also known as succinate dehydrogenase (SDH), which is highly conserved in all eukaryotes[12], exists at the crossroad between TCA cycle[13] and oxidative phosphorylation[14]. It consists of four nuclear-coded subunits, namely SDHA, SDHB, SDHC, and SDHD. Functionally, SDHA consists of the SDH catalytic site with flavin adenine dinucleotide, while SDHB consists of three 'Fe−S' clusters that transfer electrons from SDHA to the ubiquinone (UbQ) site. SDHC and SDHD are inner membrane proteins anchoring SDHA and SDHB complex on the mitochondrial inner membrane and contribute to the formation of UbQ site[14]. Complex II can generate mitochondrial reactive oxygen species (mtROS) at high rates from the flavin site even at normal substrate concentration[15]. Reactive oxygen species (ROS) plays a complex dual role in regulating cell longevity[16,17]. It causes oxidative stress, resulting in the accumulation of damaged macromolecules and loss of physiological integrity. It also acts as modulators in signaling pathways that promote longevity when the increment of ROS is in a modest level[18−22]. Whether ROS plays an advantageous or invasive role is determined by its level, species, time, target and place[16].

MitoK-ATP channels and complex II both play important roles in ischemic preconditioning[23]. Some inhibitors of complex II such as 3-nitropropionic acid, atpenin A5, and malonate can activate mitoK-ATP[24,25], whereas diazoxide, which can open mitoK-ATP channel, also acts as complex II inhibitor[26]. Although evidences suggest a close correlation between mitoK-ATP channels and mitochondrial complex II, both functionally[26−28] and pharmacologically[23], the relationship between them was remain to be studied. Interestingly, sulfonylureas, which inhibits mitoK-ATP channel, have the same chemical scaffold to diazoxide (a mitoK-ATP channel opener and complex II inhibitor), but the effect of sulfonylureas on mitochondrial complex II is unclear.

The present study aimed to investigate the anti-aging effects of sulfonylureas in *C. elegans*, human lung fibroblast MRC-5 cells, and mice. Chlorpropamide was conventionally used due to its high solubility in nematode growth medium and stable efficacy. The anti-aging mechanisms of chlorpropamide were also analyzed with special emphasis on its interaction with mitoK-ATP and complex II.

2. Materials and methods

2.1. Maintenance of *C. elegans* strains

Strains were maintained at 20 °C on the standard NGM seeded with *Escherichia coli* (*E. coli*), OP50. The wild-type N2 strain was used as a reference. Other *C. elegans* strains used in this study included (name, *genotype* and origin): TK22, *mev-1 (kn1) III,* Caenorhabditis Genetrices Center; SJ4100, *zcIs13 [hsp-6p*::GFP*] V,* Caenorhabditis Genetrices Center.

2.2. Lifespan analysis

Adult worms were grown on seeded NGM plates, collected using the M9 solution, and synchronized using fresh sodium hypochlorite (0.1 mL 10 mol/L NaOH, 0.5 mL NaClO and 1.4 mL H_2O for 2 mL bleach mixture). Embryos were placed on OP50-seeded 60 mm-NGM plates and transferred to 35 mm-NGM plates (containing 200 μmol/L 5-fluoro-2′-deoxyuridine, CAS: 50-91-9, Adamas) with or without chlorpropamide (25, 100 or 400 μmol/L, CAS: 94-20-2, J&K) when worms reached the L4 stage. During adulthood, worms were transferred to new plates with chlorpropamide every three days until Day 9 of adulthood, after which they were transferred into fresh control plates every three days until all the worms died. *N*-acetyl cysteine (NAC, 1 mmol/L, diluted from 500 mmol/L water solution) treated worms were placed on agar plates for 4 generations before lifespan assays[29]. NAC containing NGM plates were prepared freshly every week. Death was defined as no body-movement response to mechanical stimulation. Worms were counted every day until all of them died. For every lifespan assay, approximately 100 worms were used.

2.3. RNAi experiment

The *E. coli* strain, HT115, expressing L4440 control vectors or vectors engineered to produce the *sdha-1/gas-1* RNAi effect was used for the RNAi experiment[30]. *E. coli* was grown in liquid LB culture medium (25 μg/mL ampicillin was added). Bacteria were seeded on the NGM plates (25 μg/mL ampicillin and 1 mmol/L IPTG were added) and dried for one day. N2 worms were transferred to the HT115-seeded NGM plates and their F1 offsprings were synchronized for lifespan assays.

For mitochondria isolation, N2 worms on L1 stage were put on NGM plates seeded with HT115 expressing L4440 control vectors or vectors engineered to produce *sdha-1/gas-1* RNAi effect. Worms were washed, transferred onto NGM plate with DMSO/100 μmol/L chlorpropamide seeded with bacteria when they reached L4, and kept until they reached day 3 of adulthood.

2.4. Thermotolerance assay

Synchronized worms were maintained in the same condition as in lifespan assays up to day 5 of adulthood, and the thermotolerance assay was conducted as described in a previously reported procedure[31]. Briefly, worms were incubated at 35 °C for 10 h after which living worms were counted every two hours until all worms died. Approximately 100 worms were counted.

2.5. Thrashing speed assay

Thrashing speed assay was conducted on worms on Days 3, 8, and 12 of adulthood that were raised in a same condition as in lifespan assays[32]. Briefly, worms were transferred into M9 buffer for 30 s' balance. Then their body-bends in another 30 s were counted. A body bend was defined as the deviation of the centerline of the worm's body. Approximately 20 worms were counted in every group.

2.6. Pumping rates assay

Pumping rate assay was conducted as previously described[33]. Synchronized worms were raised on OP50-seeded plates and the pharyngeal pumping rate of roughly 15 animals was counted under a dissection microscope.

2.7. Cell viability assay

Cell viability assay was conducted using the Cell Counting Kit-8 (CCK-8, Beyotime). Cells were seeded into 96-well plates and incubated with chlorpropamide from 0 to 400 μmol/L for 72 h. The CCK-8 solution was added into the wells and incubated at 37 °C for 2 h. The absorbance at 450 nm was measured by a Synergy H1 Hybrid Multi-Mode Reader (Bio-Tek Instruments).

2.8. Senescence-associated β-galactosidase (SA-β-gal) staining

MRC-5 cells were cultured in MEM culture medium until replicatively senescent. SA-β-gal were stained using the Cell Senescence β-galactosidase Staining Kit (Beyotime). After incubating with DMSO, 200 μmol/L chlorpropamide or 100 μmol/L metformin for 3 days, aged cells were washed using PBS and fixed using the fixative liquid offered by the kit for 15 min. Next, the dyeing liquid was freshly prepared as per the product manual. Cells were stained in a 37 °C incubator overnight. The next day, cells were stained by DAPI and photographed using an ECLIPSE Ts2R (Nikon)[34]. Three to five photos were taken for every well.

In doxorubicin-induced (Dox-induced) senescence assays, cells were incubated with 2 nmol/L doxorubicin for seven days to induce senescence. Afterward, MEM culture medium containing doxorubicin was removed and MEM with DMSO, 200 μmol/L chlorpropamide, and 100 μmol/L metformin was added and incubated as described above. The percentage of SA-β-gal positive cells was calculated and statistically analyzed.

2.9. ATP measurement

About 150 worms were collected in 1.5 mL EP centrifuge tubes and washed thrice using the M9 buffer, leaving about 100 μL M9 in tubes after centrifuging. Precipitates were frozen in liquid nitrogen for 2 min and then put into water baths at 60 °C for 2 min. This step was repeated five times till the worms were split completely. Then the tubes were cooked in a boiling pot for 25 min, cooled on ice, and centrifuged (4 °C, 10 min, 11,000×*g*). The supernatant was transferred into new centrifuge tubes and diluted 4 × by M9 buffer. ATP levels were measured using the CellTiter-Glo® Luminescent Cell Viability Assay (Promega), while protein values were quantified using the BCA Protein Quantification Kit (Yeason). ATP levels were normalized by the protein values[35].

2.10. Mitochondrial membrane potential (MMP) measurement

MMP measurements were conducted both in worms and normal human hepatic cells (HL-7702) cells.

For worms, about five N2 worms of the L4 stage were placed on 35 mm NGM plates containing 100 μmol/L chlorpropamide for 7 days. Worms were stained using the mitochondrial membrane potential assay kit with JC-1 (Beyotime) overnight. The next day, worms were paralyzed with 25 mmol/L levamisole, transferred onto a 3% agar pad on glass slides, and photographed under a Leica TCR 6500 (Leica) at 63 × oil immersion objective, and 2 × zoom in[36]. All photographs were analyzed using ImageJ, where the light intensity of a 180-pixel circle on the pharyngeal bulb was measured. Mitochondrial membrane potential was quantified by the ratio of the intensity of red and green light.

For cells, MMP was measured using TMRE (CAS: 115532-52-0, Invitrogen) and Mitotracker Green (Yeasen)[37]. Briefly, cells were cultured in 12-well plates and incubated with DMSO or 200 μmol/L chlorpropamide for 3 days. Before the assay, the culture medium was transferred into RPMI-1640 culture medium containing 13.3 nmol/L TMRE and 200 nmol/L Mitotracker Green and incubated for 20 min in a CO_2 incubator at 37 °C. Cells were washed with PBS for 2 times and digested using trypsin−EDTA solution (Yeason) for 2 min. Then cells were washed, collected, and loaded into CytoFLEX LX (Beckman Coulter). Data were collected in FITC channel (for Mitotracker Green) and PE channel (for TMRE) by 488 nm and 561 nm excitation.

2.11. Mitochondrial isolation

N2 worms were used for mitochondrial isolation. Adult worms were collected in M9 buffer and washed at least 3 times to clear the bacteria. Cold mitochondria isolation buffer [MHSE; 70 mmol/L sucrose, 210 mmol/L mannitol, 5 mmol/L HEPES, 1 mmol/L EGTA, and 0.5% (*w*/*v*) fatty acid-free bovine serum albumin (BSA), pH 7.2] was added and washed once on ice. All

contents were moved into a Dounce homogenizer and homogenized with 10 more strokes. After that, mitochondria were isolated by differential centrifugation, at 1500×*g* for 5 min and 8000×*g* for 15 min at 4 °C. The mitochondria were then washed using isolation buffer once and were ready for other assays.

2.12. *mtROS level measurement*

Staining of isolated mitochondrial mtROS levels was measured using CytoFLEX LX (Beckman Coulter)[38]. Mitochondrial assay solution [MAS, 3 × ; 210 mmol/L sucrose, 660 mmol/L mannitol, 30 mmol/L KH_2PO_4, 15 mmol/L $MgCl_2$, 6 mmol/L HEPES, 3 mmol/L EGTA, and 0.6% (*w*/*v*) fatty acid-free BSA, pH 7.2] was used for staining. Rotenone (2 μmol/L), malonate (10 mmol/L), and antimycin A (4 μmol/L) were used as inhibitors of mitochondrial complexes I, II, and III, respectively. Mitochondria were isolated by the method described earlier. Succinate (10 mmol/L) and mitochondrial inhibitors were incubated with MitoSOX (1 μmol/L) and mitochondria in MAS (diluted to 1 ×, pH 7.2) at room temperature (20 °C) for 1 h. Afterward, mitochondria were washed by MAS with substrate and inhibitors to clear the surplus dye, resuspended in MAS with substrate and inhibitors, and measured using CytoFLEX LX (Beckman Coulter).

mtROS level of MRC-5 cells was measured using Synergy H1 Hybrid Multi-Mode Reader (Bio-Tek Instruments). Cells were incubated with or without chlorpropamide for 1, 3, 6, 9, 12, and 24 h. These cells were then washed by PBS, stained by MitoSOX (5 μmol/L) for 30 min, washed by PBS again, and measured using a Synergy H1 Hybrid Multi-Mode Reader (Bio-Tek Instruments). 12 wells were measured for each group and MitoTracker® Green FM (200 nmol/L) was used for normalization.

2.13. *Oxygen consumption rate (OCR) assay*

Oxygen consumption was measured using a Seahorse XFe96 Analyzer (Agilent) at 20 °C similar to that described in an earlier study[39]. 15 worms on Day 3 of adulthood, treated with or without chlorpropamide (100 μmol/L) as described in lifespan assay, were transferred into each well of a 96-well microplate containing 200 μL M9 buffer with 6 wells per group. Basal respiration was measured for a total of 90 min, at 9-min intervals that included a 3-min mix, a 3-min time delay, and a 3-min measurement.

Oxygen consumption of HL-7702 cells was measured using a Seahorse XFe96 Analyzer (Agilent) at 37 °C[40]. Cells were cultured in 100 mm dishes with DMSO/chlorpropamide (200 μmol/L) for two days and seeded in XF96 V3 Cell Culture Microplates (Agilent) at 10,000 cells/well over night before the experiment. Succinate (10 mmol/L) with rotenone (2 μmol/L) was added to MAS with 0.2% (*w*/*v*) BSA as substrates. ADP (final concentration, 4 mmol/L), oligomycin (final concentration, 2.5 μg/mL), FCCP (final concentration, 1 μmol/L) and antimycin A (final concentration, 4 μmol/L) was added into different ports of Seahorse cartage. For permeabilization of cells, 0.001% digitonin was used. Each experimental group was analyzed using three or four replicates.

2.14. *Dox-induced senescence in mice*

All animals were maintained at the department of laboratory animal science, Fudan University (contract No. DF848). Animal procedures were carried out according to the National Institutes of Health guidelines. Male C57BL/6N mice over 10 weeks of age were used for the doxorubicin experiments. 5 mg/kg doxorubicin was intraperitoneally injected on Day 0 and Day 10 of the experiment, the mice were given metformin/chlorpropamide dissolved in drinking water from Day 15 and sacrificed on Day 38. A whole blood sample was collected and spun for 20 min at 900×*g*. The supernatants were collected and sent to KingMed Diagnostics, Shanghai, China for aspartate aminotransferase and alanine aminotransferase measurement.

2.15. *qPCR*

mRNA of mice liver and worms was extracted using the Total RNA Isolation Kit (Omega), then reverse transcription to cDNA was done using the Hifair II 1st Strand cDNA Synthesis Kit (gDNA digester plus, Yeason). Quantitative PCR was performed using the Hieff qPCR SYBR Green Master Mix (No Rox, Yeason). The primers used are listed as follows: *Gapdh*, forward: GTGGCAAAGTGGAGATTGTTG; reverse: AGTCTTCTGGGTGGCAGTGAT. *P21*, forward: AGCAAAGTGTGCCGTTGTCT; reverse: AGAAATC TGTCAGGCTGGTC. *tba-1*, forward: TCAACACTGCCAT CGCCGCC; reverse: TCCAAGCGAGACCAGGCTTCAG. *sdha-1*, forward: ACCGATGGAAAAATTTACCAGC; reverse: CCATGATGAGATCTAGGGCAAA. *gas-1*, forward: GTCTCGATTACGT CTCCATGAT; reverse: GCTCTTGTTGGGATGTCAATAC.

2.16. *Western blot analysis*

Mice liver was homogenated in RIPA lysis buffer (strong, Yeason) added with General Protease Inhibitor Cocktail (Absin) and PMSF (Tansoole), and desaturated using 3 × SDS loading buffer (CST). Protein extracts were separated on 12% sodium dodecyl sulfate-polyacrylamide gel electrophoresis, transferred to nitrocellulose filter membrane, and blocked with 5% milk powder in 0.02% Tween in TBS for 1 h. Membranes were incubated with specific monoclonal antibodies for P21 (sc-6246, Santa Cruz), γ-H2AX (ab81299, Abcam), and GAPDH (60004-1-lg, Proteintech) overnight at 4 °C. Immunocomplexes were visualized using Peroxidase AffiniPure Goat Anti-Mouse IgG (H + L) (33201ES60, Yeason) and peroxidase-conjugated goat anti-rabbit IgG (H + L) (33101ES60, Yeason), followed by enhanced chemoluminescence (New Cell & Molecular Biotech). Quantification of the grey value was done using ImageJ.

2.17. *SDH activity measurement*

Isolated mitochondria and HL-7702 cell lysate was used for SDH activity measurement. Succinate dehydrogenase activity was measured by the reduction of the artificial electron acceptor 2,6-dichlorophenol-indophenol at 600 nm as described in an earlier study[41]. For assay buffer, 20 mmol/L succinate, 53 μmol/L 2,6-dichlorophenol-indophenol, 10 μmol/L EDTA and 0.01 mg/mL ubiquinone was diluted in 10 × phosphate buffer saline, and adjusted to pH 7.2. Rotenone (2 μmol/L), antimycin A (4 μmol/L) and NaN_3 (1/1000 dilution) was used as inhibitors of other mitochondria complexes. For worms, isolated mitochondria of DMSO/chlorpropamide (100 μmol/L) treated worms on Day 3 of adulthood was used. For cells, RIPA lysis buffer (strong) (Yeason) with PMSF (Tansoole) and Protease Inhibitor Cocktail (Servicebio) was used to lysis cells treated with DMSO/chlorpropamide (200 μmol/L) for three days. All samples were added to the assay solution in cuvettes and warmed at 30 °C for 3 min, mixed, and immediately put into a Double Beam Spectrophotometer U-2910

(HITACHI) for measurement. An absorbance change of 5 min at 600 nm was used for calculation. Protein values were quantified using the BCA Protein Quantification Kit (Yeason).

2.18. NADH dehydrogenase activity measurement

HL-7702 cells were treated with DMSO/chlorpropamide (200 μmol/L) for three days. The NADH dehydrogenase activity was measured by the oxidation of NADH at 340 nm as described earlier[42]. For assay buffer, NADH (0.1 mmol/L), BSA (3 mg/mL), ubiquinone (0.06 mmol/L) and antimycin A (4 μmol/L) was diluted by 5 × PBS and adjusted to pH 7.5. Cell lysates were used for the assay, and the absorbance change of 3 min at 340 nm was used for calculation. Protein value was quantified using BCA Protein Quantification Kit (Yeason).

2.19. Fumarate assay

Fumarate was measured using the Fumaric Acid ELISA kit (Jonln). To describe briefly, worms were collected, homogenated in M9 solution, and spun for 5 min at 12,000×*g* at 4 °C. The supernatants were used for fumarate measurement according to the manufacturer's protocol. After the stop solution was added, the fumarate level was measured using a Synergy H1 Hybrid Multi-Mode Reader (Bio-Tek Instruments) for absorbance at 450 nm.

2.20. Blood glucose assay

Food was removed from the cages on Day 37 of the experiment for 12 h-fasted. On Day 38 of the experiment, blood samples were obtained from the tail vein and the glucose levels were estimated using a GA-type 3 glucometer (Sinocare).

2.21. hsp-6p::GFP microscopy

Mitochondrial unfolded protein response was determined using *hsp-6p*::GFP (SJ4100, *zcIs13 [hsp-6p::GFP] V*) expressing worms. *cco-1* RNAi was used as positive control. Briefly, worms on Day 3 of adulthood was paralyzed, mounted on glass slides with 3% agar pad and photographed under an ECLIPSE Ts2R (Nikon) with 4 × objective.

2.22. Determination of chlorpropamide bioavailability in mice

Chlorpropamide was diluted in 5% DMSO+95% Di water at a concentration of 0.5 mg/mL for IV and 2 mg/mL for PO. A total of 18 C57BL/6N mice were used. Blood was collected at time points 1, 5, 15, 30 min, 1, 2, 4, 8, and 24 h *via* the jugular vein cannula, placed into chilled tubes containing K_2-EDTA as the anticoagulant, and centrifuged at a temperature of 4 °C, at 6800×*g*, for 6 min to collect plasma. At time points 5, 30 min, 2 and 8 h, separate cohorts of animals were sacrificed and their livers were collected. Samples were analyzed by HPLC−MS/MS. The protocol was approved by the Institutional Animal Care and Use Committee (Shanghai Medicilon Inc., Shanghai, China), and Shanghai Medicilon Inc. is accredited by the National Institutes of Health Office of Laboratory Animal Welfare (https://olaw.nih.gov/home.htm) and Association for Assessment and Accreditation of Laboratory Animal Care (www.aaalac.org).

2.23. Statistics

All assays were conducted with at least three independent replicates. Data were analyzed using GraphPad Prism 8.3.0 statistical program. Significance of the data were analyzed by Student's *t*-test, and were represented as mean ± standard error of mean (SEM), except for assays mentioned specifically. A P value < 0.05 was statistically significance.

3. Results

3.1. Chlorpropamide has an anti-aging effect on worms and human lung fibroblast MRC-5 cells

To discover the best option for anti-aging compounds, 1386 marketable drugs were screened using the *C. elegans* lifespan model. We found all four sulfonylureas, namely chlorpropamide (Fig. 1A, Supporting Information Table S1), glimepiride (Supporting Information Fig. S2A), glibenclamide (Supporting Information Fig. S2B) and tolbutamide (Supporting Information Fig. S2C) prolong the lifespan of the wild type worms (N2), suggestive of the anti-aging effects of sulfonylureas on *C. elegans*. Chlorpropamide was chosen for further study because it dissolves more easily in NGM and has a stable life-extension effect (Supporting Information Table S1).

On further analysis, it was found that chlorpropamide administration improved the survival rate of N2 worms in heat stress conditions (Fig. 1B) along with the thrashing speed in older worms (Fig. 1C), which indicates that chlorpropamide can potentially improve the healthspan of nematodes[43]. The possibility of a change in food-intake behavior by chlorpropamide was excluded, because it had no significant impact on pharyngeal pumps (Fig. 1D). We also tested whether the anti-aging effects of chlorpropamide were conserved in human cells. The results showed that chlorpropamide increased cell viability significantly at concentrations of 200 μmol/L while remaining non-toxic at concentrations up to 400 μmol/L (Supporting Information Fig. S2D). Also, the proportion of cells positive for SA-β-gal was significantly reduced in the groups treated with chlorpropamide (200 μmol/L) or metformin (100 μmol/L) compared to the control group (Fig. 1E). These results imply that chlorpropamide has conservative anti-aging effects on both worms and replicatively senescent human cells.

3.2. Chlorpropamide relieves Dox-induced senescence in vitro and in vivo

Doxorubicin can induce cellular senescence which was evident from elevated SA-β-gal activity and the increased expression of cyclin-dependent kinase inhibitor P21 which promotes cell−cycle arrest in senescent cells[44]. To investigate whether chlorpropamide can mitigate the Dox-induced senescence *in vitro*, the number of SA-β-gal positive cells was counted. Metformin was used as a positive control because of its evolutionary conservative anti-aging effects in human cells, worms, and mice[34,45,46] and ability to alleviate Dox-induced toxicity[47,48]. The results show that the number of SA-β-gal positive senescent cells increased significantly after adminstration with 2 nmol/L doxorubicin for 7 days, and both metformin and chlorpropamide were able to block this increase in MRC-5 cells (Fig. 1F).

Further, whether chlorpropamide can minimize this Dox-induced senescence in mice was examined. C57BL/6N mice

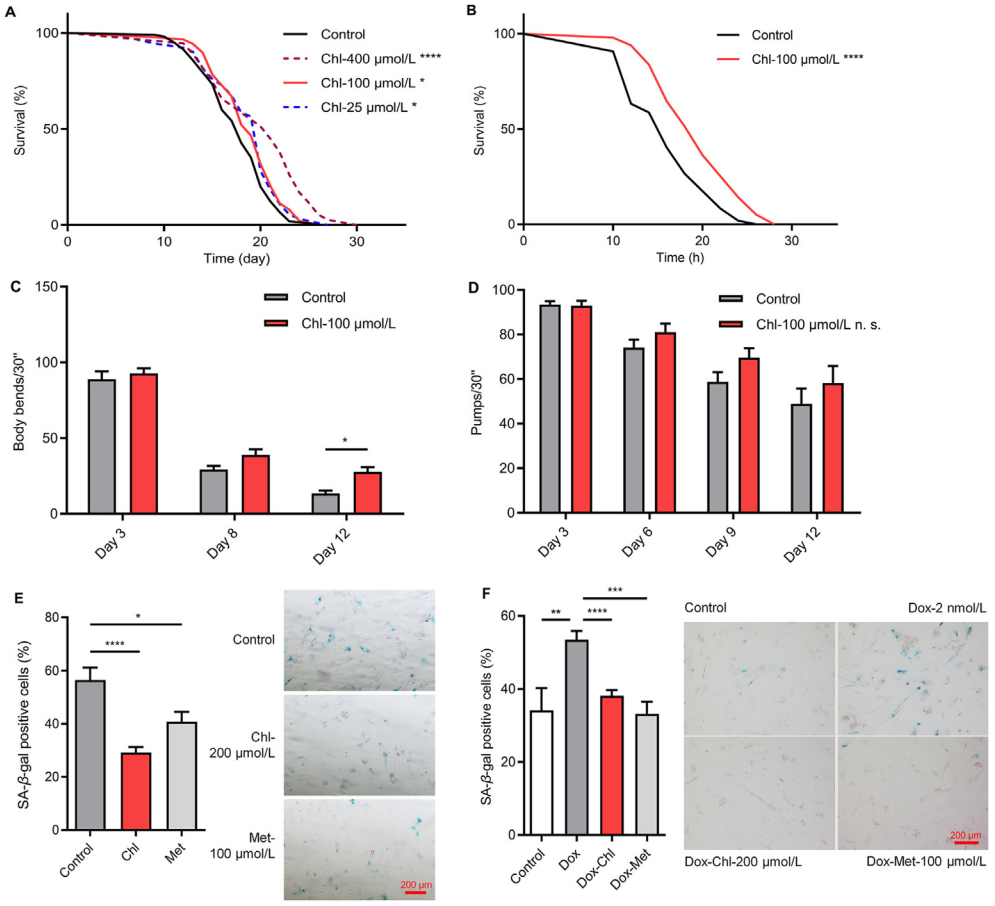

Figure 1 Chlorpropamide (Chl) delays aging in worms and MRC-5 human fibroblast cells. (A) Survival curves of N2 worms treated with Chl (0/400/100/25 μmol/L) (n = 105/111/88/92) under 20 °C. (B) Survival curves of N2 worms treated with Chl (0/100 μmol/L) (n = 109/99) under 35 °C. (C) and (D) Thrashing speed (n = 19) (C) and pharyngeal pumping rate (n = 15) (D) of N2 worms under Chl (0/100 μmol/L) treatment. (E) and (F) The senescence-associated β-galactosidase positive rate of replicatively senescent (E) and doxorubicin-induced (Dox-induced) senescent (F) MRC-5 cells under Chl (200 μmol/L) and metformin (Met) (100 μmol/L) treatment. All assays were triplicated. In (A) and (B) data were compared using the log-rank (Mantel−Cox) test. In (C)−(F) data are shown as mean ± SEM and compared using two-way ANOVA (C, D) and Students' t-test (E, F). *P < 0.05, **P < 0.01, ***P < 0.005, ****P < 0.001, n.s., not significant.

were given different concentrations of chlorpropamide (3 and 10 mg/kg) and metformin (20 mg/kg) in their drinking water for 23 days after doxorubicin (5 mg/kg) was injected intraperitoneally on Day 0 and Day 10 (Fig. 2A). Doxorubicin is known to be hepatotoxic, impairing the liver function at a dose of 10 mg/kg in mice, as observed by increased levels of serum aspartate aminotransferase and alanine aminotransferase[49]. However, the results of the current investigation show that the doxorubicin injection did not cause significant hepatotoxicity when the dose was reduced to 5 mg/kg (Fig. 2B and C). We tested the distribution of chlorpropamide to liver at 10 mg/kg and its bioavailability. The level of chlorpropamide in the liver rose to more than 10 μg/g in 5 min after intragastrical administration, showing its ability to distribute in liver at 10 mg/kg (Supporting Information Fig. S3A). The bioavailability profile illustrates characteristics of oral administration of chlorpropamide in mice, including fast absorption and slow elimination (Supporting Information Fig. S3B and Table S2). In addition, chlorpropamide and metformin at the dose used in present study did not significantly decrease the blood glucose level (Supporting Information Fig. S4A).

The transcription of *P21* as detected by RT-QPCR was significantly increased in the liver of Dox-treated mice (Fig. 2D). Whereas, administration of chlorpropamide and metformin both significantly decreased this Dox-induced transcriptional upregulation of *P21*. The change in P21 protein level was consistent with that of the *P21* mRNA levels (Fig. 2E). γ-H2AX is a marker for the DNA-damage foci, also related to senescence[50,51]. We measured the γ-H2AX protein levels in mice liver and found them to be significantly upregulated after doxorubicin injection and downregulated by chlorpropamide and metformin administration (Fig. 2F). Hence, these results also add to the evidence pointing to a reversal of *in vivo* Dox-induced senescence by chlorpropamide.

3.3. *Chlorpropamide increases the mitochondrial electrical potential*

Since sulfonylureas are also described as inhibitory to mitoK-ATP channels located in the inner mitochondrial membrane that prevents the decrease in MMP brought by mitoK-ATP channel openers[6,52], the effects of chlorpropamide on MMP were studied using the dual-emission potential-sensitive dye JC-1. A significant increase in the red/green fluorescent ratio in the chlorpropamide-treated worms was observed suggesting a higher MMP (Fig. 3A).

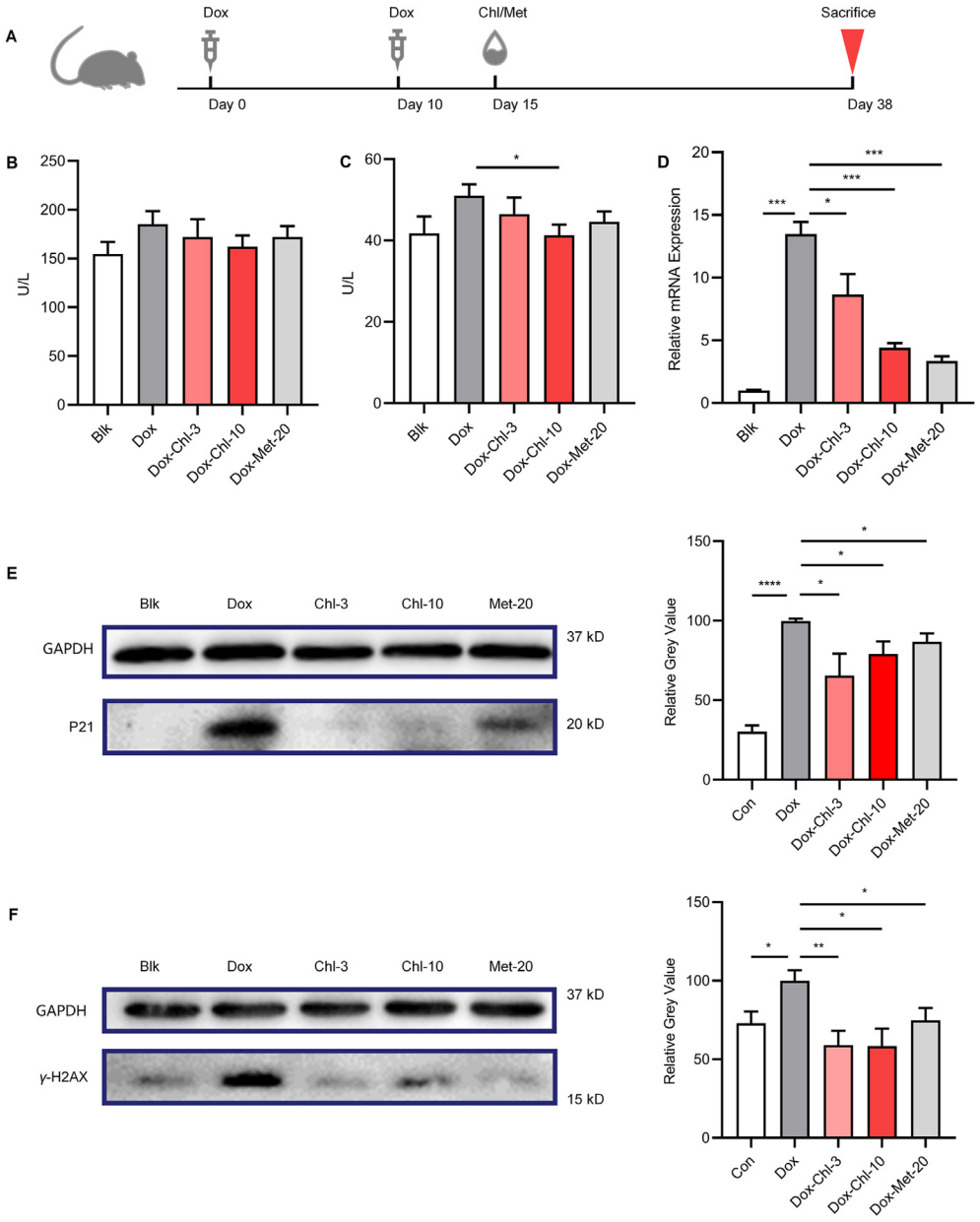

Figure 2 Chl relieves Dox-induced senescence in mice. (A) Diagram illustrating the experiments of doxorubicin and then Met/Chl administration in mice. (B) and (C) Aspartate aminotransferase (B) and alanine aminotransferase (C) levels in mice serum after doxorubicin injection with Chl (0/3/10 mg/kg) (n = 13/12/13) and Met (20 mg/kg) (n = 13) in drinking water. (D) Relative mRNA level of *P21* in mice liver after doxorubicin injection, with or without Chl (3/10 mg/kg) and Met (20 mg/kg) in drinking water. (E) and (F) Western blot of P21 (E) and γ-H2AX (F) using mice liver after doxorubicin injection with or without Chl (3/10 mg/kg) and Met (20 mg/kg) in drinking water. In (B, C) assays were conducted using the serum of more than 8 mice. In (D)−(F) assays were triplicated. All data were compared using the Student's t-test and shown as mean ± SEM. $^{*}P < 0.05$, $^{**}P < 0.01$, $^{***}P < 0.005$, $^{****}P < 0.001$, n.s., not significant.

ATP levels of worms on Day 8 of adulthood were also measured because an MMP-electrochemical gradient is essential for ATP synthesis[53]. Consequently, significantly increased ATP levels were observed in the chlorpropamide-treated worms (Fig. 3B). In addition, the OCR of the chlorpropamide-treated worms was significantly decreased (Fig. 3C), which may because of the inhibition of potassium influx into the mitochondria by chlorpropamide. This leads to less oxygen consumption needed to maintain MMP, a key indicator of mitochondrial health and function[54]. Furthermore, the up-regulated fluorescence of the *hsp-6p*::GFP (Supporting Information Fig. S4B), which is used as an indicator for the unfolded protein response in the mitochondria[55], was absent.

Then normal human hepatic cells (HL-7702) were used to test the effects of chlorpropamide on mitochondria in human cells, because chlorpropamide can resist senescence in the liver of mice (Fig. 2). A CCK-8 assay was conducted and found chlorpropamide did not show toxicity up to 400 μmol/L on HL-7702 cells (Fig. 4A). MMP level and OCR after three days' chlorpropamide treatment was detected. MMP level observed in chlorpropamide

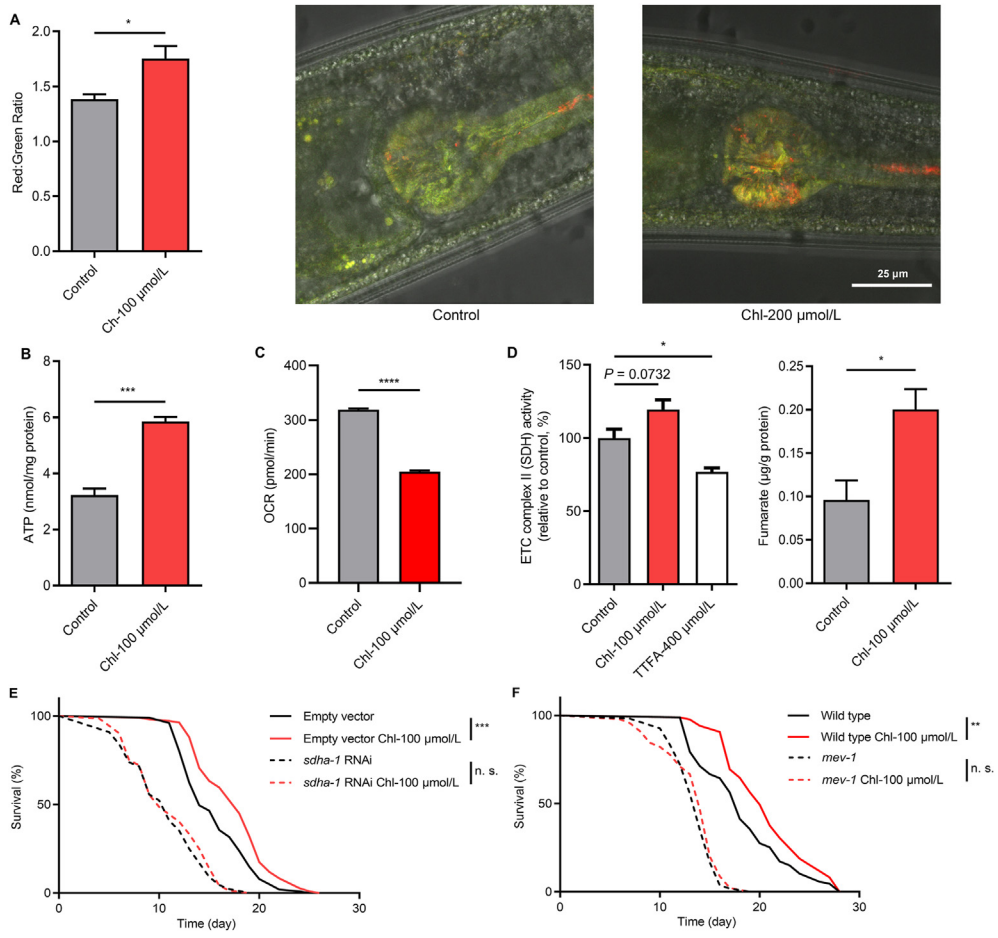

Figure 3 Chl extends the lifespan of worms through mitoK-ATP channels and mitochondrial complex II. (A) JC-1 red: green fluorescence ratio in worm pharyngeal pump on Day 8 of adulthood after DMSO/Chl (100 μmol/L) treatment ($n = 5$). The JC-1 red/green fluorescence of the worm pharyngeal pump was photographed under a Leica confocal microscope. (B) ATP level of whole worm lysis after 8 days DMSO/Chl (100 μmol/L) treatment. (C) The oxygen consumption rate of N2 worms after 3 days' DMSO/Chl (100 μmol/L) treatment. (D) Succinate dehydrogenase activity and fumarate level of N2 worms after 3 days' DMSO/Chl (100 μmol/L) treatment. (E) Survival curves of N2 worms feeding HT115 with control vector/*sdha-1* RNAi bacteria after 0/100 μmol/L Chl treatment (control vector, $n = 101/109$; *sdha-1* RNAi, $n = 88/72$). (F) Survival curves of *mev-1* (*kn1*) *III* mutant worms treated with Chl (0/100 μmol/L) (N2, $n = 87/85$; *mev-1* (*kn1*) *III*, $n = 54/45$). All assays were conducted more than twice. In (A)−(D), data were compared using Student's *t*-test and shown as mean ± SEM. In (E) and (F), data were compared using the log-rank (Mantel−Cox) test. $^*P < 0.05$, $^{**}P < 0.01$, $^{***}P < 0.005$, $^{****}P < 0.001$, n.s., not significant.

(200 μmol/L) treated cells increased significantly (Fig. 4B). The basal respiration in chlorpropamide treated cells was significantly reduced (Fig. 4C), which was accordance with the result observed in worms (Fig. 3C). State III respiration is defined as ADP-stimulated respiration in the presence of saturating substrate. State IV respiration is defined as oxygen consumption when ADP is exhausted, which is a proton leak dependent respiration[56]. A decrease of OCR in state IV respiration was observed in chlorpropamide treated groups (Fig. 4E). This finding supports our hypothesis, that chlorpropamide block the physiological opening of mitoK-ATP channels, therefore prevent proton leak dependent oxygen consumption caused by dissipation of MMP through K^+/H^+ transporters[6,52,57] (Supporting Information Fig. S1). As state III respiration is consist of proton leak dependent respiration and ATP synthases derived respiration, state III respiration were also found decreased in chlorpropamide treated cells (Fig. 4D).

3.4. *Chlorpropamide prolongs the lifespan of C. elegans through complex II*

Since mitoK-ATP channels are closely correlated with the mitochondrial complex II, we examined whether complex II is essential for chlorpropamide to increase the lifespan of *C. elegans*. HT115 bacteria expressing the *sdha-1* (human *SDHA* in *C. elegans*) dsRNA was used to knock-down *sdha-1* transcription. Interestingly, it was found that chlorpropamide had no lifespan-extending effect in the worms fed with *sdha-1* RNAi bacteria (Fig. 3E, Supporting Information Fig. S5C). Similarly, chlorpropamide did not affect the lifespan of the *sdhc-1* (human *SDHC* in *C. elegans*) mutant TK22 *mev-1(kn1) III* worms (Fig. 3F). So, we tested the impact of chlorpropamide on SDH activity and its enzymatic transformation product, fumarate. We found that chlorpropamide upregulated SDH enzyme activity ($P = 0.0732$)

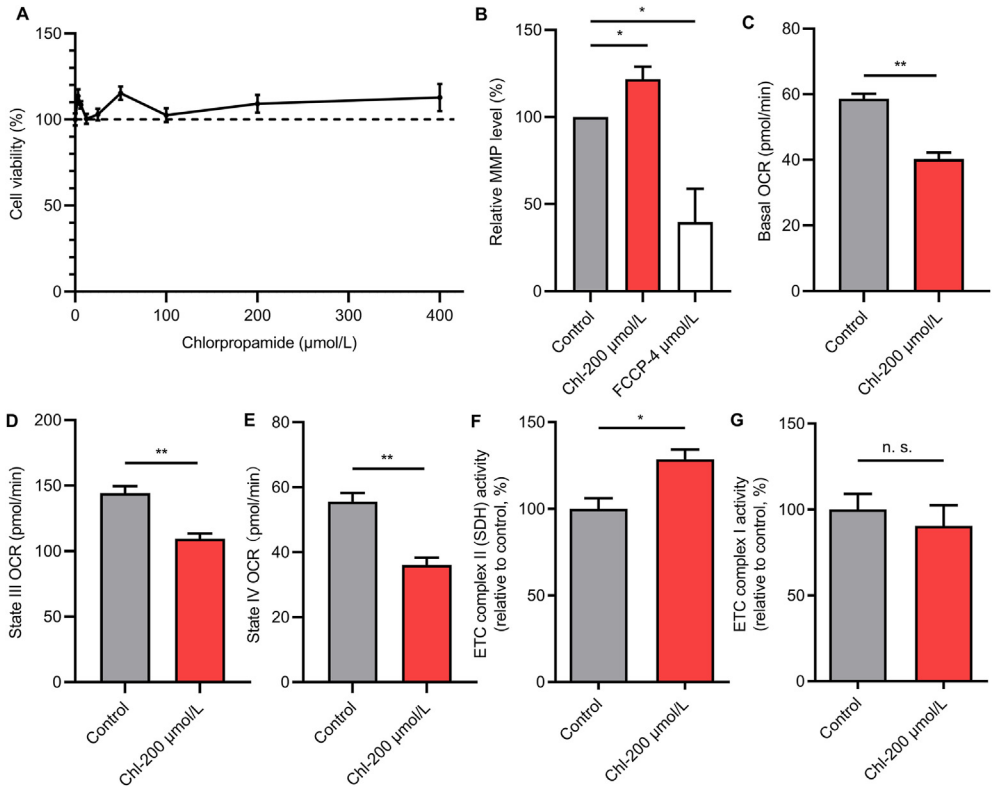

Figure 4 The effect of Chl is conservative in human cells. (A) CCK-8 tests on HL-7702 cells performed with Chl treatment of different concentration. (B) Relative mitochondrial membrane potential level (%) in HL-7702 cells after DMSO/Chl (200 μmol/L) treatment. (C)−(E) Oxygen consumption rate of basal (C), state III (D) and state IV (E) respiration in HL-7702 cells after DMSO/Chl treatment. (F) and (G) Enzymatic activity of mitochondrial complex II (succinate dehydrogenase) (F) and mitochondrial complex I (NADH dehydrogenase) (G) in HL-7702 cells after 3 days' DMSO/Chl (200 μmol/L) treatment. All assays were triplicated, compared using Student's *t*-test and shown as mean ± SEM. $^*P < 0.05$, $^{**}P < 0.01$, n.s., not significant.

and fumarate levels significantly (Fig. 3D), proposing that chlorpropamide may enhance SDH activity of complex II and thus extend the lifespan through complex II. Then we further investigated the effect of chlorpropamide on the enzymatic activity of mitochondrial complex I (NADH dehydrogenase) and II (SDH) in HL-7702 cells. We observed SDH activity was increased (Fig. 4F) and NADH dehydrogenase activity was unchanged (Fig. 4G) in chlorpropamide treated groups, which suggested the consistent effect of chlorpropamide on mitochondrial complex II in human cells and nematodes.

3.5. Chlorpropamide prolongs the lifespan via an increase in mtROS levels

Since complex II can generate ROS, both by a physiological and pathological signal, mtROS level was measured by MitoSOX staining. Mitochondria were isolated from worms and then stained with MitoSOX, following which the upregulation of mtROS level in chlorpropamide-treated worms was observed (Fig. 5A). Different mitochondrial complex inhibitors were incubated with the isolated mitochondria from chlorpropamide-treated worms. The results show that chlorpropamide induced an increase in mtROS level in the rotenone (complex I inhibitor) and antimycin A (complex III inhibitor) treated group, but not in the malonate (complex II inhibitor) treated group (Fig. 5A), suggesting that the chlorpropamide-induced upregulated mtROS levels can be attributed to the complex II-derived respiration. The effects of chlorpropamide on complex I and complex II were confirmed by genetic silencing of *gas-1* and *sdha-1* expression (Supporting Information Fig. S5A−S5C). *sdha-1* RNAi eliminates the induction of mtROS after chlorpropamide treatment (Supporting Information Fig. S5A), which is consistent with our results using mitochondrial complex inhibitors (Fig. 5A). We observed the increase of mtROS induced by chlorpropamide in worms fed with *gas-1* RNAi bacteria was not significant (Supporting Information Fig. S5A), which might because mitochondrial complex I dysfunction can enhance mitochondrial complex II derived respiration[58], and therefore weaken the significance of chlorpropamide induced mtROS level. Taken togather, these results confirmed that upregulation of mtROS levels may due to mitochondrial complex II derived respiration affected by chlorpropamide.

The MitoSOX fluorescence intensity was also examined in the MRC-5 cells, and an upregulated mtROS level at the beginning of chlorpropamide treatment was observed, which reached a peak at 6 h after chlorpropamide addition (Fig. 5B). Then, the mtROS levels started to decrease, and a level less than the control group was attained after 12 h. This change in mtROS levels suggests that moderate ROS production activates certain signaling pathways that promote longevity[38,59].

Moreover, to investigate whether the upregulation of mtROS was necessary for chlorpropamide to influence the lifespan, worms treated with the antioxidant regent, NAC were examined. Surprisingly, the NAC-treatment eliminated the chlorpropamide-induced

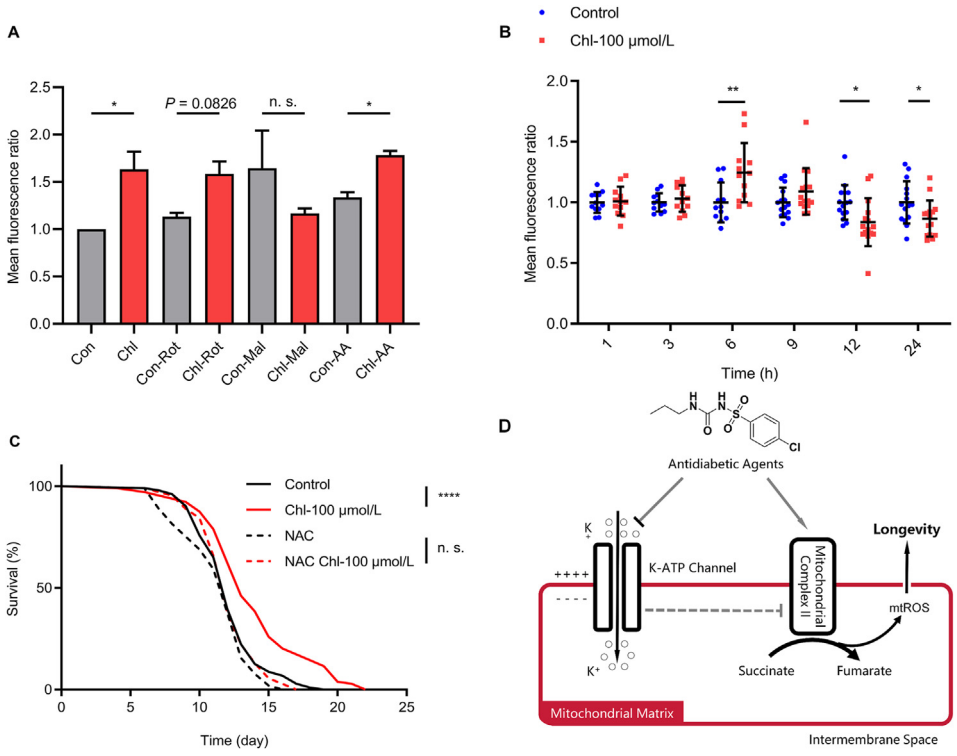

Figure 5 Chl extends lifespan *via* increasing mitochondrial reactive oxygen species. (A) and (B) Mitochondrial reactive oxygen species of isolated mitochondria of worms (A) and MRC-5 cells (B) treated with DMSO/Chl. For worms, 100 μmol/L Chl was used. Rotenone, malonate and antimycin A were used as inhibitors of mitochondrial complexes I, II and III. For human cells, 200 μmol/L Chl was used. (C) Survival curves of N2 worms grown on control or *N*-acetyl cysteine (1 mmol/L) plate treated with DMSO/Chl (100 μmol/L) (control plates, $n = 103/104$; *N*-acetyl cysteine plates, $n = 103/108$). (D) Diagram illustrating the anti-aging mechanisms of Chl. All assays were triplicated. In (A) and (B) data were compared using Student's *t*-test and shown as mean ± SEM. In (C), data were compared using the log-rank (Mantel−Cox) test. $^{*}P < 0.05$, $^{**}P < 0.01$, $^{****}P < 0.001$, n.s., not significant.

lifespan extension in worms (Fig. 5C). These results indicate that chlorpropamide extends lifespan through a mtROS-dependent pathway (Fig. 5D).

4. Discussion

Although sulfonylureas are now recommended in World Health Organization's guidelines for lowering blood glucose levels in patients with type 2 diabetes mellitus ahead of newer glucose-lowering medications, there have been concerns regarding the cardiovascular safety of sulfonylureas for more than 50 years[2]. These concerns were first raised after a study conducted under the University Group Diabetes Program reported an increased risk of both all-cause and cardiovascular mortality observed in a small number of patients treated with a first-generation sulfonylurea, tolbutamide, compared with placebo[60]. Afterward, some observational studies and meta-analyses of sulfonylurea trials associated with cardiovascular risks and mortality showed conflicting results[60,61]. Results from large, multicentric randomized controlled trials such as the United Kingdom Prospective Diabetes Study and ADVANCE confirmed the microvascular benefits of sulfonylureas as well as the potential long-term anti-mortality benefits[62]. The risks *versus* benefits of sulfonylureas are debatable and hence, the present study about the anti-aging effects of sulfonylureas on senescence in normal animals may add to this existing body of knowledge. In addition, the dosage of chlorpropamide for anti-aging effect was 10 mg/kg, much lower than 200 mg/kg for hypoglycemic effect in mice. Chlorpropamide (10 mg/kg) administration had no significant effect on blood glucose level of nondiabetic mice (Supporting Information Fig. S4A)[63,64]. The effect occurred below the effective dose for hypoglycemic use enables chlorpropamide to function as a potential anti-aging regent without causing serious side effects.

Sulfonylureas besides inhibiting the K-ATP channels located on the cell membrane thereby increasing insulin secretion, also inhibit the activity of K-ATP channels located on the inner mitochondrial membrane whose physiological functions need to be further studied[4,6]. In the present study, we found that chlorpropamide significantly increased both MMP and ATP levels in nematodes which occurs possibly by inhibiting the outflow of potassium ions from the intermembrane space to the mitochondrial matrix (Fig. 3A, B, and Supporting Information Fig. S1). Since both MMP and ATP losses are assumed to be pathognomic of mitochondrial dysfunction in aged cells[65,66], the elevation of MMP and ATP level in chlorpropamide-treated worms suggests a positive influence of chlorpropamide in maintaining a healthier living condition in the worms. It was observed that chlorpropamide upregulated SDH enzyme activity along with the level of its enzymatic transformation product, fumarate. Additionally, SDHA-1 and SDHC-1 of complex II are required for chlorpropamide-induced life-extension of nematodes. To the best of our knowledge, this is the first study analyzing a lifespan-extending mechanism regulating the mitochondria complex II by a small molecular compound. But whether the mechanism of action of chlorpropamide on mitochondrial complex II is direct or indirect is yet to be discovered. The possibility of both ways, that

chlorpropamide directly activates complex II or affects the activity of complex II by acting on the mitoK-ATP channel, exists (Fig. 5D).

ROS is involved in redox signaling in physiological conditions, while it can also cause oxidative stress and induce apoptosis[67]. In this study, a moderate elevation of mtROS levels in worms and MRC-5 cells was seen which may activate the protective mechanisms leading to increased stress resistance and contributing to lifespan extension[68]. Furthermore, this chlorpropamide-induced lifespan extension in worms can be partially eliminated by NAC-treatment, reaffirming the role of chlorpropamide in affecting the animal's lifespan through a mtROS dependent pathway. Also, the mtROS level measured using different inhibitors and gene silencing of mitochondrial complexes, and the enzymatic activity of mitochondrial complexes I and II indicate that the upregulation of mtROS level was achieved from the complex II-derived respiration. We don't know whether upregulating SDH activity leads to the increase of mtROS levels because complex II functions as a source as well as a suppressor or enhancer of ROS-production by other respiratory chain complexes depending on the physiological situation.

5. Conclusions

This study successfully demonstrated chlorpropamide as a potential anti-aging compound in *C. elegans*, Dox-induced senescent human cells and mice. The mechanisms of these effects were studied in worms and human cells. It was observed that SDH activity of complex II, the level of MMP and mtROS in chlorpropamide-treated worms and cells were increased. Also, complex II and increased mtROS levels were required for lifespan extension of chlorpropamide, revealing the interaction of chlorpropamide with mitochondrial complex II, directly or indirectly *via* mitoK-ATP channels to increase the production of mtROS as a pro-longevity signal.

Acknowledgments

Financial support for this research provided by the National Natural Science Foundation of China (22037002 and 81772689), the Program for Professor of Special Appointment (Eastern Scholar TP2018025, China) at Shanghai Institutions of Higher Learning, the Innovative Research Team of High-level Local Universities in Shanghai, and the Chinese Special Fund for State Key Laboratory of Bioreactor Engineering (2060204, China). Strains of *Caenorhabditis elegans* were provided by the CGC, which is funded by NIH Office of Research Infrastructure Programs (P40 OD010440).

Author contributions

Jian Li and Zelan Hu contributed to the design of the research, manuscript writing, and provided financial support. Zhifan Mao and Wenwen Liu performed the experiments and analyzed the data. Yunyuan Huang helped to analyze the data. Tianyue Sun helped to perform mice experiments. Keting Bao and Jiali Feng helped to perform lifespan screening. Alexey Moskalev contributed to the revision of the manuscript. All the authors have approved the final version of the manuscript.

Conflicts of interest

The authors declare no conflicts of interest.

Appendix A. Supporting information

Supporting data to this article can be found online at https://doi.org/10.1016/j.apsb.2021.08.007.

References

1. Sanjay K, Yashdeep G. Sulfonylureas. *J Pakistan Med Assoc* 2015;**65**:101−4.
2. Webb DR, Davies MJ, Jarvis J, Seidu S, Khunti K. The right place for sulphonylureas today. *Diabetes Res Clin Pract* 2019;**157**:107836.
3. Martin GM, Kandasamy B, DiMaio F, Yoshioka C, Shyng SL. Anti-diabetic drug binding site in a mammalian K_{ATP} channel revealed by Cryo-EM. *Elife* 2017;**6**:e31054.
4. Sturgess N, Cook D, Ashford M, Hales CN. The sulphonylurea receptor may be an ATP-sensitive potassium channel. *Lancet* 1985;**326**:474−5.
5. Isao I, Hideki N, Kuki K, Tomihiko H. ATP-sensitive K^+ channel in the mitochondrial inner membrane. *Nature* 1991;**352**:244−7.
6. Paggio A, Checchetto V, Campo A, Menabo R, Di Marco G, Di Lisa F, et al. Identification of an ATP-sensitive potassium channel in mitochondria. *Nature* 2019;**572**:609−13.
7. Paucek P, Mironova G, Mahdi F, Beavis AD, Woldegiorgis G, Garlid KD. Reconstitution and partial purification of the glibenclamide-sensitive, ATP-dependent K^+ channel from rat liver and beef heart mitochondria. *J Biol Chem* 1992;**267**:26062−9.
8. Garlid KD, Paucek P, Yarov-Yarovoy V, Sun X, Schindler PA. The mitochondrial K_{ATP} channel as a receptor for potassium channel openers. *J Biol Chem* 1996;**271**:8796−9.
9. Adam S. The ATP-regulated K^+ channel in mitochondria: five years after its discovery. *Acta Biochim Pol* 1996;**43**:713−9.
10. Roper J, Ashcroft FM. Metabolic inhibition and low internal ATP activate K-ATP channels in rat dopaminergic substantia nigra neurones. *Pflügers Archiv* 1995;**430**:44−54.
11. Winkle DMV, Chien GL, Wolff RA, Soifer BE, Kuzume K, Davis RF. Cardioprotection provided by adenosine receptor activation is abolished by blockade of the K_{ATP} channel. *Am J Physiol* 1994;**266**:H829−39.
12. Sun F, Huo X, Zhai Y, Wang A, Xu J, Su D, et al. Crystal structure of mitochondrial respiratory membrane protein complex II. *Cell* 2005;**121**:1043−57.
13. Cecchini G. Function and structure of complex II of the respiratory chain. *Annu Rev Biochem* 2003;**72**:77−109.
14. Bezawork-Geleta A, Rohlena J, Dong L, Pacak K, Neuzil J. Mitochondrial complex II: at the crossroads. *Trends Biochem Sci* 2017;**42**:312−25.
15. Quinlan CL, Orr AL, Perevoshchikova IV, Treberg JR, Ackrell BA, Brand MD. Mitochondrial complex II can generate reactive oxygen species at high rates in both the forward and reverse reactions. *J Biol Chem* 2012;**287**:27255−64.
16. Meng J, Lv Z, Zhang Y, Wang Y, Qiao X, Sun C, et al. Precision redox: the key for antioxidant pharmacology. *Antioxidants Redox Signal* 2021;**34**:1069−82.
17. Schaar CE, Dues DJ, Spielbauer KK, Machiela E, Cooper JF, Senchuk M, et al. Mitochondrial and cytoplasmic ROS have opposing effects on lifespan. *PLoS Genet* 2015;**11**:e1004972.
18. Hekimi S, Lapointe J, Wen Y. Taking a "good" look at free radicals in the aging process. *Trends Cell Biol* 2011;**21**:569−76.
19. Hwang AB, Ryu EA, Artan M, Chang HW, Kabir MH, Nam HJ, et al. Feedback regulation *via* AMPK and HIF-1 mediates ROS-dependent longevity in *Caenorhabditis elegans*. *Proc Natl Acad Sci USA* 2014;**111**:E4458−67.

20. Benjamin D, Stefan B, Fabian S, Tommy S, Martin H, Uwe W, et al. Mitochondrial oxidative stress impairs energy metabolism and reduces stress resistance and longevity of *C. elegans*. *Oxid Med Cell Longev* 2019;**2019**:6840540.
21. Seung-Jae L, Hwang Ara B, Cynthia K. Inhibition of respiration extends *C. elegans*' lifespan *via* reactive oxygen species that increase HIF-1 activity. *Curr Biol* 2010;**20**:2131−6.
22. Vikram A, Anish R, Kumar A, Tripathi DN, Kaundal RK. Oxidative stress and autophagy in metabolism and longevity. *Oxid Med Cell Longev* 2017;**2017**:3451528.
23. Ardehali H, Chen Z, Ko Y, Mejía-Alvarez R, Marbán E. Multiprotein complex containing succinate dehydrogenase confers mitochondrial ATP-sensitive K^+ channel activity. *Proc Natl Acad Sci U S A* 2004; **101**:11880−5.
24. Wojtovich AP, Brookes PS. The endogenous mitochondrial complex II inhibitor malonate regulates mitochondrial ATP-sensitive potassium channels: implications for ischemic preconditioning. *Biochim Biophys Acta* 2008;**1777**:882−9.
25. Wojtovich AP, Brookes PS. The complex II inhibitor atpenin A5 protects against cardiac ischemia−reperfusion injury *via* activation of mitochondrial K_{ATP} channels. *Basic Res Cardiol* 2009;**104**:121−9.
26. Hanley PJ, Mickel M, Loffler M, Brandt U, Daut J. K_{ATP} channel-independent targets of diazoxide and 5-hydroxydecanoate in the heart. *J Physiol* 2002;**542**:735−41.
27. Riepe MW, Niemi WN, Megow D, Ludolph AC, Carpenter DO. Mitochondrial oxidation in rat hippocampus can be preconditioned by selective chemical inhibition of succinic dehydrogenase. *Exp Neurol* 1996;**138**:15−21.
28. Edalat A, Schulte-Mecklenbeck P, Bauer C, Undank S, Krippeit-Drews P, Drews G, et al. Mitochondrial succinate dehydrogenase is involved in stimulus-secretion coupling and endogenous ROS formation in murine beta cells. *Diabetologia* 2015;**58**:1532−41.
29. Zarse K, Schmeisser S, Groth M, Priebe S, Beuster G, Kuhlow D, et al. Impaired insulin/IGF1 signaling extends life span by promoting mitochondrial L-proline catabolism to induce a transient ROS signal. *Cell Metabol* 2012;**15**:451−65.
30. Kamath RS, Martinez-Campos M, Zipperlen P, Fraser AG, Ahringer J. Effectiveness of specific RNA-mediated interference through ingested double-stranded RNA in *Caenorhabditis elegans*. *Genome Biol* 2001; **2**. research0002.
31. Huang XB, Wu GS, Ke LY, Zhou XG, Wang YH, Luo HR. Aspirin derivative 5-(bis(3-methylbut-2-enyl)amino)-2-hydroxybenzoic acid improves thermotolerance *via* stress response proteins in *Caenorhabditis elegans*. *Molecules* 2018;**23**:1359.
32. Iwasa H, Yu S, Xue J, Driscoll M. Novel EGF pathway regulators modulate *C. elegans* healthspan and lifespan *via* EGF receptor, PLC-gamma, and IP3R activation. *Aging Cell* 2010;**9**:490−505.
33. Yin JA, Gao G, Liu XJ, Hao ZQ, Li K, Kang XL, et al. Genetic variation in glia-neuron signalling modulates ageing rate. *Nature* 2017;**551**:198−203.
34. Fang J, Yang J, Wu X, Zhang G, Li T, Wang X, et al. Metformin alleviates human cellular aging by upregulating the endoplasmic reticulum glutathione peroxidase 7. *Aging Cell* 2018;**17**:e12765.
35. Wu S, Lei L, Song Y, Liu M, Lu S, Lou D, et al. Mutation of hop-1 and pink-1 attenuates vulnerability of neurotoxicity in *C. elegans*: the role of mitochondria-associated membrane proteins in Parkinsonism. *Exp Neurol* 2018;**309**:67−78.
36. Luz AL, Godebo TR, Bhatt DP, Ilkayeva OR, Maurer LL, Hirschey MD, et al. From the cover: arsenite uncouples mitochondrial respiration and induces a warburg-like effect in *Caenorhabditis elegans*. *Toxicol Sci* 2016;**152**:349−62.
37. Dingley S, Chapman KA, Falk MJ. Fluorescence-activated cell sorting analysis of mitochondrial content, membrane potential, and matrix oxidant burden in human lymphoblastoid cell lines. *Methods Mol Biol* 2012;**837**:231−9.
38. Yang W, Hekimi S. A mitochondrial superoxide signal triggers increased longevity in *Caenorhabditis elegans*. *PLoS Biol* 2010;**8**:e1000556.
39. Riekelt H, Houtkooper, Laurent M, Dongryeol R, Norman M, Elena K, Graham K, et al. Mitonuclear protein imbalance as a conserved longevity mechanism. *Nature* 2013;**497**:451−7.
40. Zhang B, Chu W, Wei P, Liu Y, Wei T. Xanthohumol induces generation of reactive oxygen species and triggers apoptosis through inhibition of mitochondrial electron transfer chain complex I. *Free Radic Biol Med* 2015;**89**:486−97.
41. Ramachandran PV, Savini M, Folick AK, Hu K, Masand R, Graham BH, et al. Lysosomal signaling promotes longevity by adjusting mitochondrial activity. *Dev Cell* 2019;**48**:685−96. e5.
42. Lee H, Ko E, Shin S, Choi M, Kim KT. Differential mitochondrial dysregulation by exposure to individual organochlorine pesticides (OCPs) and their mixture in zebrafish embryos. *Environ Pollut* 2021; **277**:115904.
43. Rollins JA, Howard AC, Dobbins SK, Washburn EH, Rogers AN. Assessing health span in *Caenorhabditis elegans*: lessons from short-lived mutants. *J Gerontol A Biol Sci Med Sci* 2017;**72**:473−80.
44. Meredith AM, Dass CR. Increasing role of the cancer chemotherapeutic doxorubicin in cellular metabolism. *J Pharm Pharmacol* 2016; **68**:729−41.
45. Onken B, Driscoll M. Metformin induces a dietary restriction-like state and the oxidative stress response to extend *C. elegans* healthspan *via* AMPK, LKB1, and SKN-1. *PLoS One* 2010;**5**:e8758.
46. Martin-Montalvo A, Mercken EM, Mitchell SJ, Palacios HH, Mote PL, Scheibye-Knudsen M, et al. Metformin improves healthspan and lifespan in mice. *Nat Commun* 2013;**4**:2192.
47. Asensio-Lopez MC, Sanchez-Mas J, Pascual-Figal DA, Abenza S, Perez-Martinez MT, Valdes M, et al. Involvement of ferritin heavy chain in the preventive effect of metformin against doxorubicin-induced cardiotoxicity. *Free Radic Biol Med* 2013;**57**:188−200.
48. Alhowail A, Almogbel Y. Metformin administration increases the survival rate of doxorubicin-treated mice. *Pharmazie* 2019;**74**:737−9.
49. Baar MP, Brandt RMC, Putavet DA, Klein JDD, Derks KWJ, Bourgeois BRM, et al. Targeted apoptosis of senescent cells restores tissue homeostasis in response to chemotoxicity and aging. *Cell* 2017; **169**:132−47. e16.
50. De Cecco M, Ito T, Petrashen AP, Elias AE, Skvir NJ, Criscione SW, et al. L1 drives IFN in senescent cells and promotes age-associated inflammation. *Nature* 2019;**566**:73−8.
51. Yang X, Yu D, Xue L, Li H, Du J. Probiotics modulate the microbiota−gut−brain axis and improve memory deficits in aged SAMP8 mice. *Acta Pharm Sin B* 2020;**10**:475−87.
52. Bednarczyk P, Kicinska A, Laskowski M, Kulawiak B, Kampa R, Walewska A, et al. Evidence for a mitochondrial ATP-regulated potassium channel in human dermal fibroblasts. *Biochim Biophys Acta Bioenerg* 2018;**1859**:309−18.
53. Friedman JR, Nunnari J. Mitochondrial form and function. *Nature* 2014;**505**:335−43.
54. Sakamuru S, Attene-Ramos MS, Xia M. Mitochondrial membrane potential assay. *Methods Mol Biol* 2016;**1473**:17−22.
55. Quiros PM, Mottis A, Auwerx J. Mitonuclear communication in homeostasis and stress. *Nat Rev Mol Cell Biol* 2016;**17**:213−26.
56. Ramani M, Miller K, Brown J, Kumar R, Kadasamy J, McMahon L, et al. Early life supraphysiological levels of oxygen exposure permanently impairs hippocampal mitochondrial function. *Sci Rep* 2019;**9**:13364.
57. Jastroch M, Divakaruni AS, Mookerjee S, Treberg JR, Brand MD. Mitochondrial proton and electron leaks. *Essays Biochem* 2010;**47**: 53−67.
58. Hawkins BJ, Levin MD, Doonan PJ, Petrenko NB, Davis CW, Patel VV, et al. Mitochondrial complex II prevents hypoxic but not calcium- and proapoptotic Bcl-2 protein-induced mitochondrial membrane potential loss. *J Biol Chem* 2010;**285**:26494−505.

59. Meng J, Lv Z, Qiao X, Li X, Li Y, Zhang Y, et al. The decay of redox-stress response capacity is a substantive characteristic of aging: revising the redox theory of aging. *Redox Biol* 2017;**11**: 365−74.
60. Riddle MC. Modern sulfonylureas: dangerous or wrongly accused?. *Diabetes Care* 2017;**40**:629−31.
61. Wexler DJ. Sulfonylureas and cardiovascular safety: the final verdict?. *J Am Med Assoc* 2019;**322**:1147−9.
62. Holman RR, Paul SK, Bethel MA, Matthews DR, Neil HAW. 10-year follow-up of intensive glucose control in type 2 diabetes. *N Engl J Med* 2008;**359**:1577−89.
63. Aderibigbe AO, Emudianughe TS, Lawal BA. Evaluation of the antidiabetic action of *Mangifera indica* in mice. *Phytother Res* 2001; **15**:456−8.
64. Rohde BH, Chiou GC. Effects of glucose on neuroblastoma *in vitro* and *in vivo*. *J Pharmacol Sci* 1987;**76**:366−70.
65. Fang EF, Scheibye-Knudsen M, Brace LE, Kassahun H, SenGupta T, Nilsen H, et al. Defective mitophagy in XPA *via* PARP-1 hyperactivation and NAD^+/SIRT1 reduction. *Cell* 2014;**157**:882−96.
66. Hongbo Z, Dongryeol R, Yibo W, Karim G, Xu W, Peiling L, et al. NAD+ repletion improves mitochondrial and stem cell function and enhances life span in mice. *Science* 2016;**352**:1436−43.
67. Qi S, Guo L, Yan S, Lee RJ, Yu S, Chen S. Hypocrellin A-based photodynamic action induces apoptosis in A549 cells through ROS-mediated mitochondrial signaling pathway. *Acta Pharm Sin B* 2019;**9**:279−93.
68. Campisi J, Kapahi P, Lithgow GJ, Melov S, Newman JC, Verdin E. From discoveries in ageing research to therapeutics for healthy ageing. *Nature* 2019;**571**:183−92.